International Journal of Multiphase Flow 37 (2011) 67–75

Contents lists available at ScienceDirect

International Journal of Multiphase Flow

journal homepage: www.elsevier.com/locate/ijmulflow

Experimental study of inverted annular film boiling in a vertical tube cooled by R-134a

Meamer El Nakla [a,*], D.C. Groeneveld [b,c], S.C. Cheng [c]

[a] Mechanical Engineering Department, King Fahd University of Petroleum & Minerals, Dhahran 31261, Saudi Arabia
[b] Thermalhydraulics Branch, Atomic Energy of Canada Limited, Chalk River, Canada K0J 1J0
[c] Department of Mechanical Engineering, University of Ottawa, Ottawa, Canada K1N 6N5

ARTICLE INFO

Article history:
Received 7 August 2009
Received in revised form 9 August 2010
Accepted 14 August 2010
Available online 19 August 2010

Keywords:
Inverted annular film boiling
Hot-patch techniques

ABSTRACT

An experimental investigation of inverted annular film boiling heat transfer has been performed for vertical up-flow in a round tube. The experiments used R-134a coolant and covered a pressure range of 640–2390 kPa (water equivalent range: 4000–14,000 kPa) and a mass flux range of 500–4000 kg m^{-2} s^{-1} (water equivalent range: 700–5700 kg m^{-2} s^{-1}). The inlet qualities of the tests ranged from −0.75 to −0.03. The hot-patch technique was used to obtain the subcooled film boiling measurements. It was found that the heat transfer vs. quality curve can be divided into four different regions, each characterized by a different mechanisms and trends. These regions are dependent on pressure, mass flux and local quality. A detailed examination of the parametric trends of the heat transfer coefficient with respect to mass flux, inlet quality, heat flux and pressure was performed; reasonably good agreement between observed trends and those reported in the literature were noted.

1. Introduction

Film boiling is a heat transfer mode during which the heated surface is separated from the liquid-phase by a vapor film. It is characterized by low heat transfer coefficients due to the poor heat transfer in the vapor film layer. Flow film boiling heat transfer is generally divided into two main regimes: (i) inverted annular flow film boiling (IAFB) at void fractions (ratio of vapor to total cross sectional flow areas) of less than 0.5, and (ii) dispersed flow film boiling (DFFB) at void fractions of greater than 0.8. The transition zone between these two regimes is called agitated or inverted slug flow regime. During IAFB, a vapor film separates the heated wall from a continuous liquid core while during DFFB the liquid is entrained in a continuous vapor core in the form small droplets. The IAFB regime has high heated surface temperatures, compared to the moderate heated surface temperatures of the DFFB regime. These high temperatures could lead to physical failure of the heated surface in water cooled systems, therefore experiments were performed in Freon R-134a at water-equivalent conditions of interest.

IAFB is important in the safety analysis of water-cooled nuclear reactors. A part of the fuel bundle can experience film boiling during a loss of coolant accident (LOCA) occurrence. This mode of heat transfer can also be encountered during a loss-of-regulation accident (LORA) when the reactor power accidentally increases. Film boiling heat transfer may also be encountered in fossil-fuel-fired boilers, cooling of various high-heat-flux devices, cryogenic systems and metallurgical processing.

2. Previous IAFB experiments

The occurrence of critical heat flux (CHF) in a heat-flux controlled system will results in a large increase in wall temperature of the heated surface. This increase might cause physical burn out of the heated surface. This is especially true for subcooled water where the heat flux at CHF is very high. Although the resulting IAFB conditions are impossible to obtain during normal operation of nuclear reactors, they could occur during a LOCA. Experiments to measure IAFB are nearly impossible to obtain using a conventional heat-flux controlled system. To overcome the difficulties associated with obtaining IAFB data, the "hot-patch" techniques are implemented. Currently there are two successfully implemented hot-patch methods (Fig. 1):

- Indirectly heated hot-patch: This experimental technique uses a cylindrical copper block brazed onto the test section, as shown schematically in Fig. 1a. The hot-patch block is heated by cartridge heaters embedded in the copper block. The power supply to the heaters is independent from the power supply used for heating the remainder of the test section. This will allow the hot-patch heat flux to exceed the critical heat flux, while the

* Corresponding author. Tel.: +966 3 8607687; fax: +966 3 8602949.
E-mail address: elnakla@kfupm.edu.sa (M.E. Nakla).

0301-9322/$ - see front matter © 2010 Elsevier Ltd. All rights reserved.
doi:10.1016/j.ijmultiphaseflow.2010.08.006

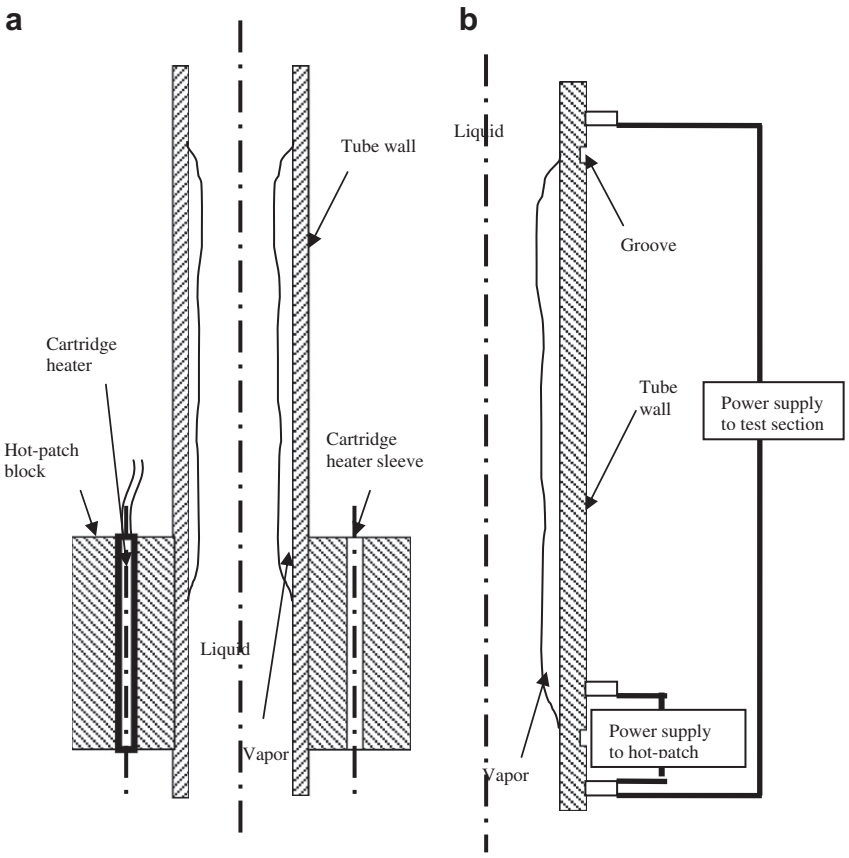

Fig. 1. Schematic diagram of test sections equipped with (a) indirectly and (b) directly heated hot-patch.

test section heat flux is still low enough to prevent failure. IAFB experiments that used indirectly heated hot-patch techniques are those of Fung (1981), Stewart (1981), Laperriere (1983), Swinnerton et al. (1988), Takenaka et al. (1989), and Hammouda et al. (1996).

- Directly heated hot-patch: In this method the wall thickness of the tube test section is reduced over a short length at both ends (a notch or groove as shown in Fig. 1b), to increase the electrical resistance of the tube at the reduced thickness location. This produces more heat flux at the notch location for the same power applied to the test section. The power to the hot-patch and the test section might be controlled separately. This method was first applied by Chen and Li (1984) to obtain IAFB data. Directly heated hot-patch experiments include those of Chen and Li (1984), Chen (1987), Chen et al. (1988, 1989), Mosaad and Johannsen (1989), and Chen et al. (1996).

IAFB experiments are more complex and are therefore less common than DFFB experiments. The ranges of these experiments are also limited to specific applications. Table 1 summarizes available IAFB experiments with the range of flow conditions of each experiment and the hot-patch technique used to obtain IAFB data.

3. Description of IAFB experiment

The experiments were performed with Freon 134a as a coolant. The Freon flow is measured by a Coriolis type flow meter with accuracy better than 0.5% (flow range 0–0.34 kg s^{-1}). The coolant flows vertically upwards through the test section, which is directly heated by a 40 V, 300 A direct current (DC) power supply. The fluid temperatures at the inlet and outlet of the test section are measured by RTDs. All sensor outputs are connected to data acquisition system and displayed on a computer monitor.

The tubular test section is made of Inconel 600, and has an inside diameter of 5.46 mm and an outside diameter of 7.54 mm. The test section is heated by a DC supplied through copper power terminals clamped tightly to the tube. The heated length of the test section is 1.20 m. The outer wall temperatures of the test section are measured by attaching 24 K-type self-adhesive thermocouples (a pair of thermocouples at each plane in 12 locations). Fig. 2 shows the test section schematic with the dimensions and the thermocouple locations.

The indirectly heated hot-patch technique is used to facilitate IAFB measurements at low powers. The copper hot-patch, shown schematically in Fig. 1a is silver-brazed to the Inconel tube near the inlet and equipped with six 200 W cartridge heaters heated by a separate alternating current (AC) power supply.

4. Experimental results and discussion

4.1. General

The experiments flow conditions cover a pressure (p) range of 640–2390 kPa (water equivalent range: 4000–14,000 kPa) and a mass flux (G) range of 500–4000 kg $m^{-2}s^{-1}$ (water equivalent range: 700–5700 kg m^{-2} s^{-1}). The inlet subcoolings and heat flux (q'') levels are varied as long as film boiling is maintained. The outer wall temperatures are measured during the experiment by K-type Chromel–Alumel thermocouples, clamped to the outside of the Inconel test section. No thermal insulation was applied to the test section due to the low heat losses. The uncertainties of directly measured quantities are summarized in Table 2. The inner wall

Table 1
Summary of subcooled and low-quality data obtained by hot-patch techniques for tube geometry.

Reference	Test fluid	Pressure (kPa)	Mass flux (kg m−2 s^{-1})	Inlet quality	Hot-patch technique[a]
Fung (1981)	Water	100	50–500	−0.131 to −0.009	Indirect
Stewart (1981)	Water	2000–9000	110–2750	−0.160 to −0.026	Indirect
Laperriere (1983)	Water	9600	1000–4500	−0.190 to 0.150	Indirect
Chen and Li (1984)	Water	100	134–646	−0.101 to 0.000	Direct
Chen (1987)	Water	1000–5500	130–920	−0.144 to 0.000	Direct
Chen et al. (1988)	Water	105–1024	25–512	−0.029 to 0.12	Direct
Swinnerton et al. (1988)	Water	200–2000	47–1010	−0.075 to −0.005	Indirect
Takenaka et al. (1989)	R-113	100	136–1280	−0.075 to −0.019	Indirect
Chen et al. (1989)	Water	410–6000	47.5–1462	−0.05 to 0.24	Direct
Mosaad and Johannsen (1989)	Water	100	50–500	−0.056 to 0.000	Direct
Chen et al. (1996)	Water	110–5830	23.9–1460	−0.056 to 0.872	Direct
Hammouda et al. (1996)	R-12, R-22 and R-134a	830–1600	530–3000	Inlet subcooling 5–28 °C	Indirect

Indirect hot-patch: using a heater block.
[a] Direct hot-patch: using a groove in the test section.

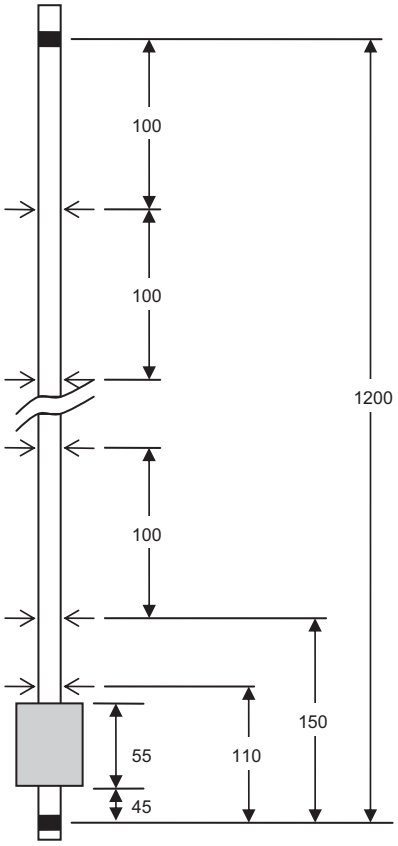

Fig. 2. Schematic diagrams of test sections and thermocouple locations.

temperatures are calculated after correcting for the temperature drop across the heated wall. Heat transfer coefficients are evaluated based on the difference between the inside wall temperature, T_w, and the saturation temperature, T_{sat}, corresponding to pressure at the outlet of the test section. The effect of pressure drop on saturation temperature is relatively small and is therefore ignored.

$$h = \frac{q''}{T_w - T_{sat}} \tag{1}$$

During the experiment, the hot-patch power is controlled such that the CHF location is at the exit of hot-patch block. This is similar to CHF experiments where CHF is measured at the exit of the test section. The average hot-patch heat flux has been found to be comparable to the corresponding CHF value using CHF look-up table of Groeneveld et al. (1996). The comparison is performed by applying fluid-to-fluid modeling technique of Ahmad (1973). This technique suggests that the boiling numbers of both a prototype and modeling fluids are equal if the quality, Reynolds number and vapor-to-liquid density ratios are equal for both fluids.

4.2. Heat transfer regions

In this study, four film boiling regions have been identified as shown in Fig. 3. Region I occurs just downstream of the hot-patch and is characterized by a sharp drop in heat transfer coefficient, *h*. In this region conduction is the dominant heat transfer mode: as the liquid core temperature increases, condensation rate decreases resulting in an increase in vapor film thickness which in turn results in a drop in heat transfer coefficient. As the liquid core temperature increases, the heat transfer rate to the liquid core decreases and the excess heat increases the evaporation rate. This results in an increase in vapor velocity and convection starts to dominate in region II. In region III, the heat transfer coefficient levels off and may show a small increase or decrease with respect to increasing quality, *x*. Region IV is again characterized by an increasing heat transfer coefficient as quality increases, presumably due to the start of DFFB regime. In this regime, evaporation rates increase with quality resulting in increased heat transfer

Table 2
Uncertainty in directly measured values.

Measured variable	Symbol	Units	Device range	Used range	Maximum uncertainty
Test section inside diameter	D	mm	5.461	5.461	UD = 0.0254 mm
Test section heated length	Lh	m	1.1	0.9–1.2	U_{Lh} = 0.001 m
Pressure	P	kPa	0–3447	635–2390	$(U_P)_{max}$ = 4.31 kPa
Mass flow rate	m	kg s^{-1}	0–0.333	0.0237–0.1523	$(U_m)_{max}$ = 0.001134 kg s^{-1}
Test section electrical voltage	U	V	0–40	0–40	$(U_U)_{max}$ = 0.241 V
Test section electrical current	I	A	0–320	0–320	$(U_I)_{max}$ = 1.93 A
Inlet temperature	Tin	°C	0–100	0–76	$(U_{Tin})_{max}$ = 0.813 °C
HFC-134a property	–	–	–	–	U_{prop}/prop = 0.005

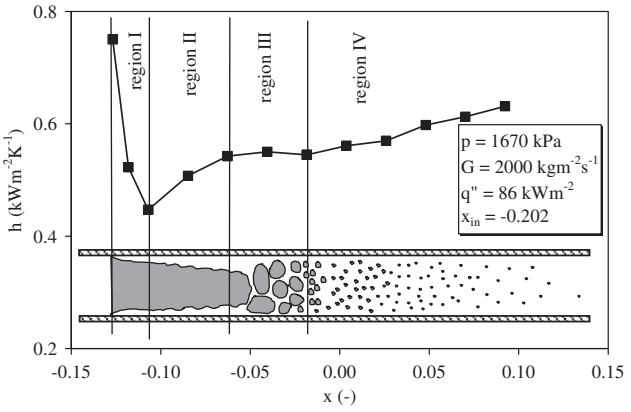

Fig. 3. Heat transfer regions during IAFB.

coefficient. It is observed that the regions I and II usually appear in the subcooled IAFB region ($x < 0$) and regions III and IV extend from the negative to the positive quality regions. The effect of the flow parameters on these four regions will be discussed in more detail in the following section.

Takenaka et al. (1989) performed steady-state IAFB experiments in a vertical tube and identified three heat transfer regions. These regions were attributed to the different flow patterns. Ishii and Denton (1988) observed similar flow patterns in their experimental study but divided the film boiling length into four regions related to the smooth, rough wavy, agitated and dispersed flow regimes (also shown in Fig. 3). Hammouda et al. (1996) classified their observations based on Ishii and Denton (1988) conclusions.

4.3. Effect of test conditions on heat transfer coefficient

4.3.1. Effect of axial location

The axial location has a strong effect heat transfer coefficient (see Fig. 4). Generally, the heat transfer coefficient decreases, then it either levels off or increases, depending on flow conditions. Although the various observations show different trends of heat transfer coefficient vs. quality or length, these trends are usually mass flux dependent and are a result of opposing effects:

- The initial decrease in heat transfer coefficient with decreasing subcooling is due to heat transfer in the IAFB region being dominated by conduction at high subcoolings: with a decrease in subcooling the vapor thickness increases, hence the resistance increases as well.
- At locations further downstream, the positive quality region is reached where convective heat transfer becomes important. For high mass velocities the vapor superheat is minimal, and an increase in quality will result in an increase in vapor velocity and hence an increase in heat transfer coefficient.
- For low mass velocities, the convection also becomes more important with an increase in quality for $x > 0$. However, because the vapor superheat also increases, the net effect of a quality increase on heat transfer coefficient h [h is generally defined as in Eq. (1)] can be very small or even negative.

The effect of various flow parameters (p, G, q'' and CHF quality, x_{DO}) on heat transfer coefficient with respect to axial location is also shown in Fig. 4. It seems that the only effect of flow parameters is to change the magnitude of heat transfer coefficient while keeping the general shape of the curve.

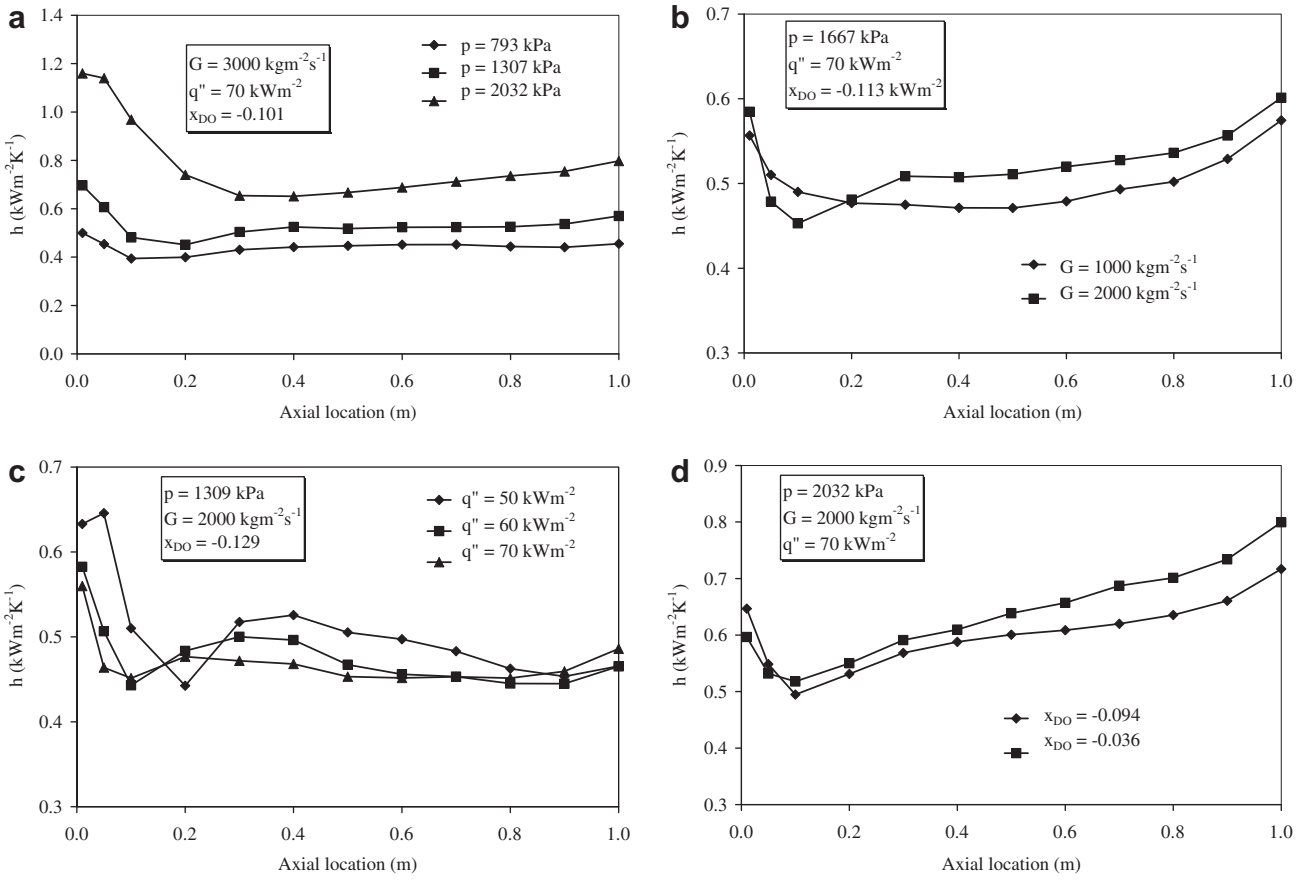

Fig. 4. Effect of axial location on heat transfer coefficient.

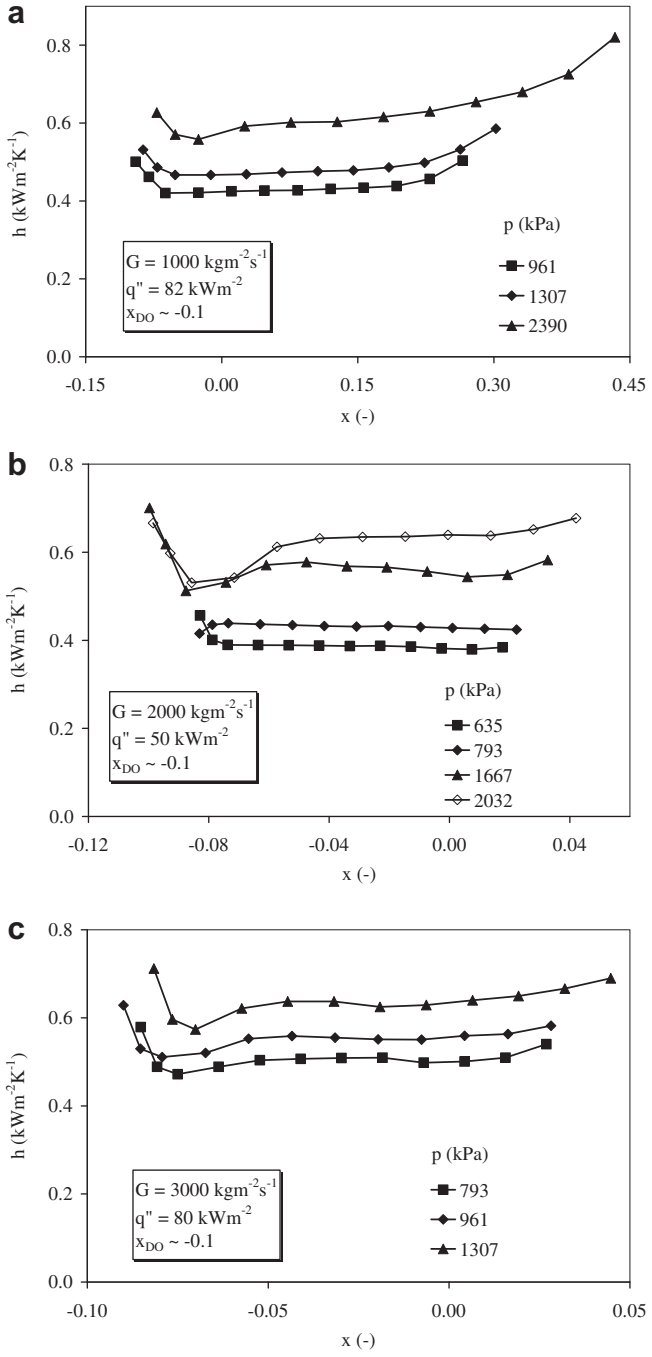

Fig. 5. Effect of pressure on heat transfer coefficient at (a) low, (b) moderate, and (c) high mass fluxes.

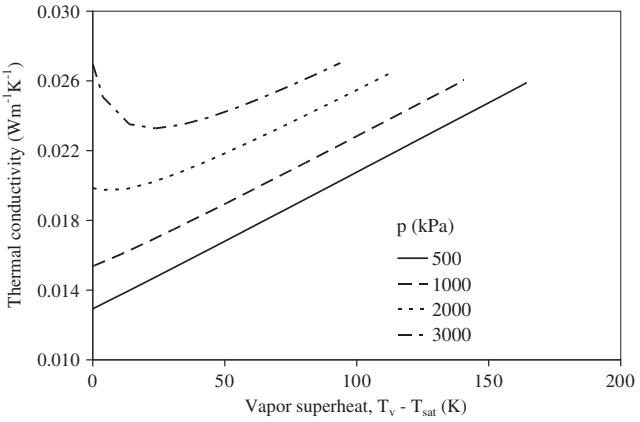

Fig. 6. Variation of vapor thermal conductivity of R-134a with pressure.

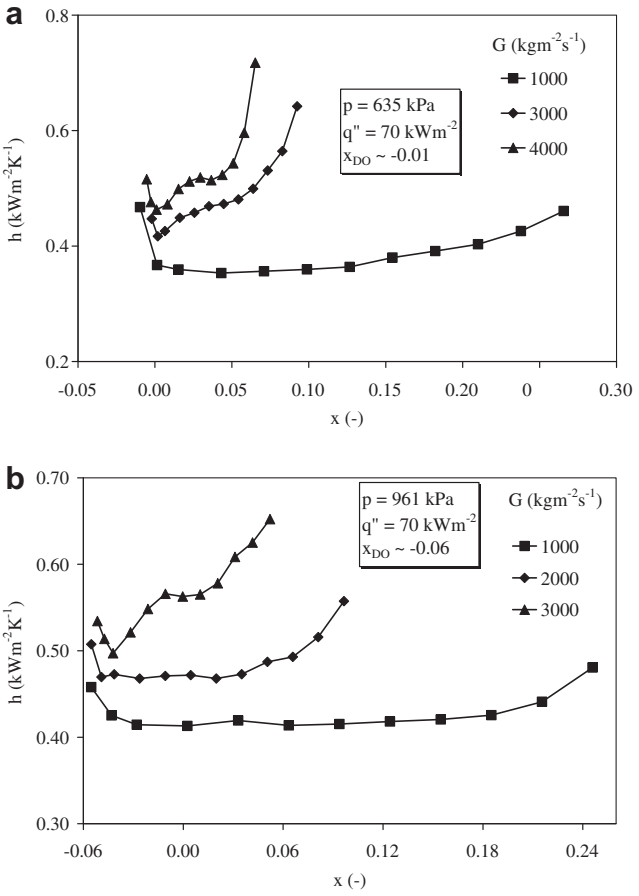

Fig. 7. Effect of mass flux on heat transfer coefficient at (a) low, and (b) moderate pressures.

4.3.2. Effect of pressure

Fig. 5 shows that the heat transfer coefficient increases with increasing pressure for low, moderate and high mass fluxes. The increase in heat transfer coefficient with pressure is primarily due to the increase in thermal conductivity of the vapor (Fig. 6).

The relation between pressure and heat transfer regions can also be identified in Fig. 5. It is observed that at lower pressures and low to moderate mass fluxes (Fig. 5a and b), heat transfer region II does not appear. At high pressures, region II appears regardless of the value of mass flux. Another observation from the figure is that at low pressures, the heat transfer coefficient following region I is almost constant (probably due to the presence of saturated inverted annular flow regime). The observed effect of pressure on heat transfer coefficient is consistent with observations by previous investigators (e.g. Hammouda et al., 1996; Stewart, 1981). Hammouda (1996) reported that at low mass flux the effect was less pronounced.

4.3.3. Effect of mass flux

A strong effect of mass flux on the heat transfer coefficient was reported in the literature by most investigators (e.g. Fung, 1981; Denham, 1984; Chen, 1987; Chen et al., 1988). Fig. 7 shows that

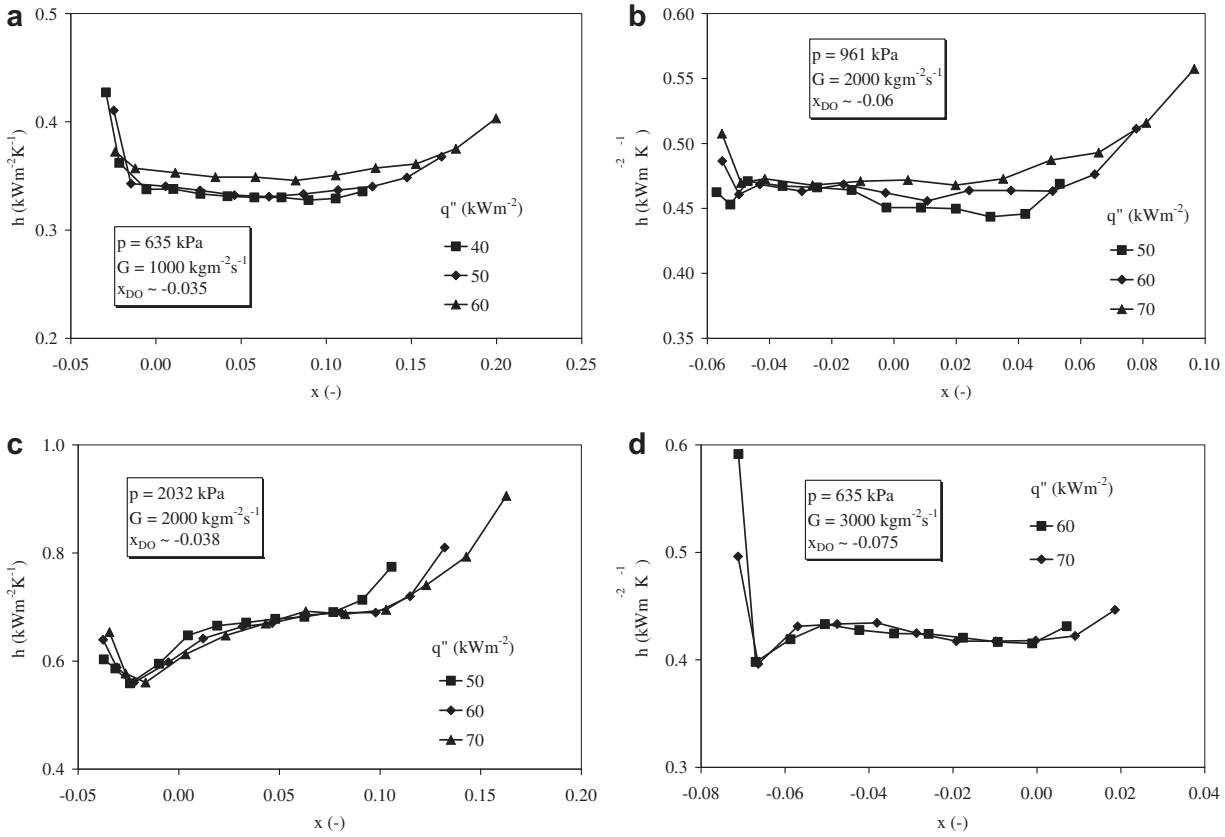

Fig. 8. Effect of heat flux on heat transfer coefficient.

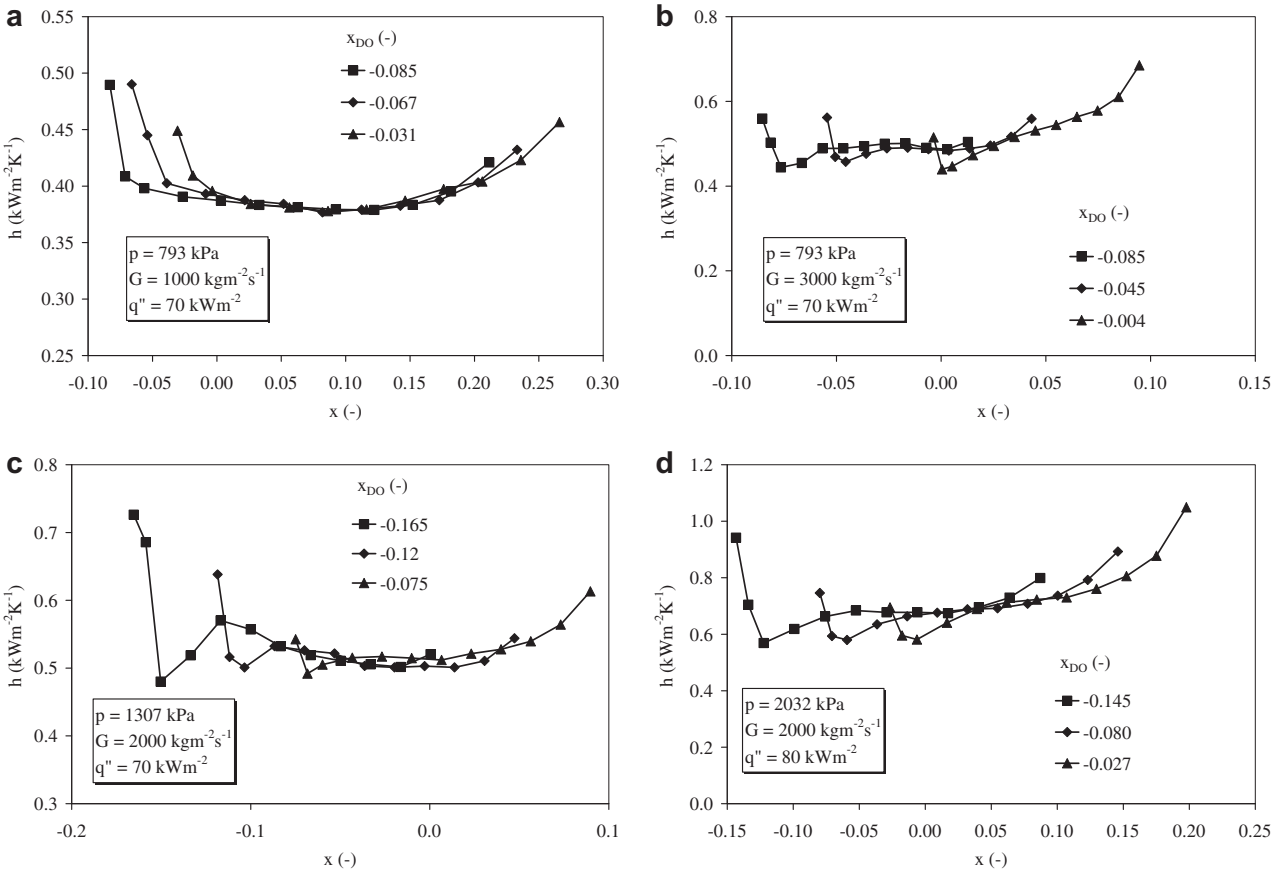

Fig. 9. Effect of inlet subcooling on heat transfer coefficient.

the observed mass flux effect agrees with the reported mass flux effect on heat transfer coefficient: an increasing mass flux always increases the heat transfer coefficient. At low mass velocities only regions III and IV appear present, but the number of regions increases as the mass flux increases. At moderate pressure, the four regions become distinctive at moderate mass flux (Fig. 7b).

As the mass flux is reduced from 3000 kg m^{-2} s^{-1} to 2000 kg m^{-2} s^{-1}, region II starts to become less pronounced and, with a further decrease to 1000 kg m^{-2} s^{-1}, this region disappears. This might be attributed to the quality range of the subcooled IAFB region. At high mass fluxes, the transition from subcooled (regions I and II which are characterized with thin vapor film) to saturated inverted annular film (region III which is characterized with higher qualities and higher vapor generation) occurs further downstream in the test section than for low mass fluxes.

4.3.4. Effect of heat flux

There is no definitive conclusion on the effect of heat flux on heat transfer coefficient. However, varying the heat flux has a weak effect on heat transfer coefficient. This effect is demonstrated in Fig. 8 for different flow conditions. In most cases, heat transfer coefficient marginally increases with increasing heat flux. There are three opposing components that can contribute to the effect of heat flux on heat transfer coefficient during subcooled IAFB:

- as the heat flux increases, the vapor layer thickness increases, and since conduction is the dominant heat transfer mode, the heat transfer coefficient drops,
- as the heat flux increases, the wall temperature increases as well and this results in a higher thermal conductivity (see later Fig. 6) and thus a higher heat transfer coefficient,
- as the vapor layer thickness increases, the velocity increases and the flow becomes turbulent, resulting in an increase in heat transfer coefficient.

The balance between these three effects determines the overall effect of heat flux on heat transfer coefficient.

At all pressures, the shape of the heat transfer coefficient vs. quality curves stays the same for all regions (regions I–IV). It was also noticed that the transition quality between regions I and II always occurred at the same quality regardless of the variation in heat flux. This same observation was made by Hammouda (1996).

A final remark on the effect of heat flux on the heat transfer coefficient is that region II is not always evident at low pressures (e.g. Fig. 8a). This might be attributed to the higher qualities at this pressure.

4.3.5. Effect of inlet subcooling

In general, the heat transfer coefficient is strongly affected by inlet subcooling at locations just downstream of the CHF location. The effect of inlet subcooling on heat transfer coefficient decreases and even vanishes as the local quality increases.

Fig. 9 shows the effect of inlet quality/subcooling on the heat transfer coefficient at different flow conditions. It is clear that as the quality increases, the heat transfer coefficient curves for different inlet qualities (keeping other flow conditions the same) converge to a single curve.

An increase in inlet subcooling shifts the transition between region I and II to lower qualities as shown in Fig. 9b–d. At moderate and high pressures and high inlet subcoolings, region IV is hardly present since the whole heat transfer coefficient curve is in the subcooled region ($x < 0$). As the inlet subcooling decreases this re-

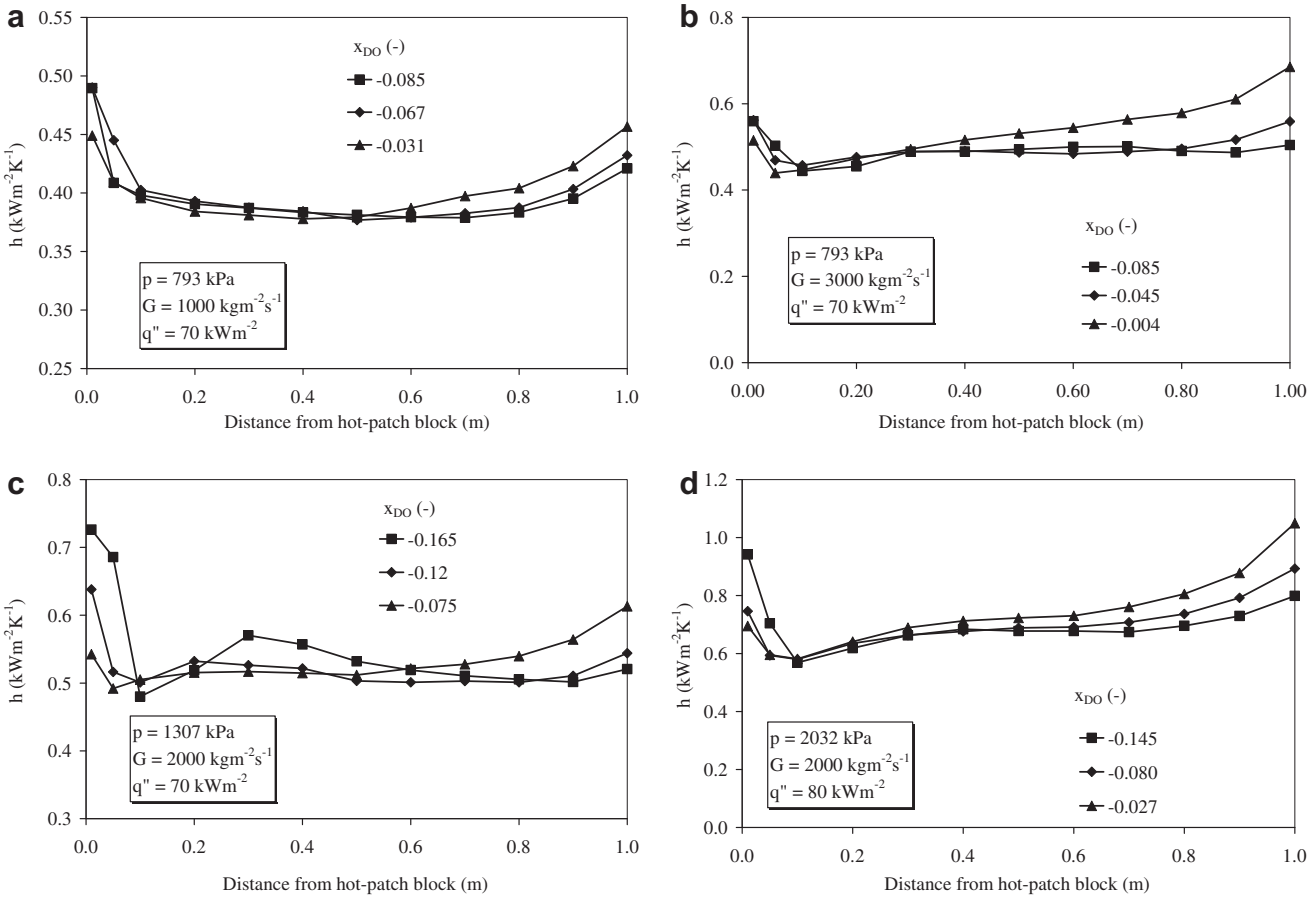

Fig. 10. Effect of inlet subcooling on heat transfer coefficient considering distance from hot-patch block.

gion starts to develop at the expense of regions II and III and becomes the dominant region as the inlet temperature approaches saturation. As explained earlier this is due to the increase in vapor generation and the change in the flow regime from subcooled inverted annular flow to saturated inverted annular flow or even to dispersed flow. Also at higher inlet subcoolings the drop in heat transfer coefficient in region I is slightly larger and the minimum heat transfer coefficient becomes smaller. This explains the large wall temperature gradient directly after critical heat flux point in highly subcooled flow.

Fig. 10 represents the same data of Fig. 9 plotted versus axial location. The figure shows that the minima in heat transfer coefficient curves coincide along the test section regardless of inlet subcooling and flow conditions. This suggests that the main contributor to this reduction in heat transfer coefficient is the entrance effect since after length to diameter ratio, L/D = 20–30, the minimum appears to have been reached.

4.3.6. Effect of hot-patch

Several runs were performed to check the hot-patch effect on wall temperature. These runs were carried out by switching off the power supplied to the hot-patch and waiting for the hot-patch temperature to drop. The temperature drop resulted in gradual rewetting of the test section. Fig. 11 shows the variation of wall temperature (and heat transfer coefficient) as the quench front moves downstream from the hot-patch towards the outlet of the test section. The figure shows that after quenching of the hot-patch, the wall temperature changes slightly. The effect of quench front propagation on heat transfer coefficient is shown in Fig. 11b. The region just downstream of the quench front (developing heat transfer region) is the most affected part of the heat transfer coefficient curve. Further downstream from the quench front, the deviation between heat transfer coefficient curves starts to disappear (fully developed heat transfer region). This effect is similar to the effect of inlet subcooling on heat transfer coefficient.

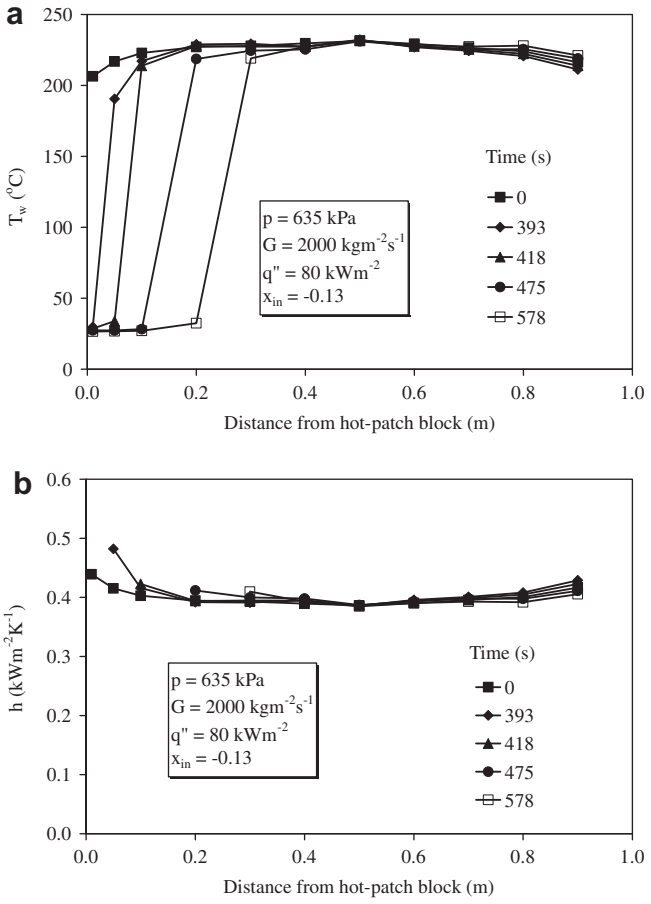

Fig. 11. Effect of quench front propagation on wall temperature and heat transfer coefficient.

5. Conclusions and final remarks

- Measurements of wall temperature and calculations of heat transfer coefficients of IAFB regime were obtained experimentally for a vertical up-flow in a circular tube using R-134a as a coolant. A total of 10,260 data points were obtained from which 6862 data points with equilibrium quality of less than 0.1. Flow conditions covered a pressure range of 640–2390 kPa (water equivalent range: 4000–14,000 kPa), a mass flux range of 500–4000 kg m^{-2} s^{-1} (water equivalent range: 700–5700 kg m^{-2} s^{-1}) and a post-CHF quality range of −0.49–1.0. The inlet qualities for which IAFB measurements could be obtained were dependent on mass flux and pressure and were within the range of −0.75 to −0.03. The hot-patch technique was used to obtain the subcooled film boiling measurements.
- Four separate IAFB heat transfer regions were identified; their boundaries depend on pressure, mass flux and quality. The general observed trend of heat transfer coefficient vs. quality is that it decreases sharply just downstream of the dryout location. The trend then varies with other flow parameters.
- Effects of varying pressure, mass flux, heat flux and inlet subcooling on IAFB heat transfer coefficient were investigated and compared to reported effects by other investigators. Generally, the heat transfer coefficient increases with increasing pressure and mass flux. The heat flux shows weak effect on heat transfer coefficient and inlet subcooling affects the heat transfer coefficient only for a short region just downstream from the CHF location.

Acknowledgement

Financial support offered by Natural Sciences and Engineering Research Council of Canada is greatly appreciated.

References

Ahmad, S.Y., 1973. Fluid to fluid modeling of CHF: a compensated distortion model. Int. J. Heat Mass Transfer 16, 641–662.

Chen, Y., 1987. Experimental study of inverted annular flow film boiling heat transfer of water. In: Wang, B.-X. (Ed.), Heat Transfer Science and Technology. Hemisphere Pub. Co., pp. 627–634.

Chen, Y., Li, J., 1984. Subcooled flow film boiling of water at atmospheric pressure. In: Chen, X.-J., Veziroglu, T.N. (Eds.), Two-Phase Flow and Heat Transfer. Hemisphere Pub. Co., pp. 141–150.

Chen, Y., Fu, X., Chen, S.P., 1988. Experimental and analytical study of inverted annular film boiling of water. In: Shah, R.K. et al. (Eds.), Experimental Heat Transfer Fluid Mechanics and Thermodynamics. Elsevier Sci. Publ., pp. 1438–1443.

Chen, Y., Wang, J., Yang, M., Fu, X., 1989. Experimental measurement of the minimum film boiling temperature of flowing water. Multiphase flow and heat transfer. In: 2nd Int. Symposium 1, pp. 393–400.

Chen, Y., Xu, H., Chen, H., 1996. Experimental results of steady-state film boiling of forced flow water. China Institute of Atomic Energy, Beijing, China, Presented at 2nd Research Coordinated Meeting of IAEA, CRP on Thermalhydraulic Relationships for AWCR, Vienna.

Denham, M.K., 1984. Inverted annular film boiling and the bromley model. AIChE Symp. Ser. 86, 13–23.

Fung, K.K., 1981. Subcooled and Low Quality Film Boiling of Water in Vertical Flow at Atmospheric Pressure. Ph.D. Thesis, University of Ottawa, Canada.

Groeneveld, D.C., Leung, L.K.H., Kirillov, P.L., Bobkov, V.P., Smogalev, I.P., Vinogradov, V.N., Huang, X.C., Royer, E., 1996. The 1995 look-up table for critical heat flux in tubes. Nucl. Eng. Des. 163, 1–23.

Hammouda, N., 1996. Subcooled Film Boiling of Referigerants in Vertical up-Flow. Ph.D. Thesis, University of Ottawa, Canada.

Hammouda, N., Groeneveld, D.C., Cheng, S.C., 1996. An experimental study of subcooled film boiling of refrigerants in vertical up-flow. Int. J. Heat Mass. Transfer 39, 3799–3812.

Ishii, M., Denton, J. P., 1988. Experimental Study of Two-Phase Flow Behaviour of the Post Critical Heat Flux Region. Japan–US Seminar on Two-Phase Flow Dynamics, Ohtsu Japan.

Laperriere, A., 1983. An Analytical and Experimental Investigation of Forced Convective Film Boiling. M.A.Sc. Thesis, University of Ottawa, Ottawa, on, Canada.

Mosaad, M., Johannsen, K., 1989. Experimental study of steady-state film boiling heat transfer of subcooled water flowing upwards in a vertical tube. Exp. Thermal Fluid Sci. 2, 477–493.

Stewart, J.C., 1981. Low Quality Film Boiling at Intermediate and Elevated Pressures. M.A.Sc. Thesis, University of Ottawa, Canada.

Swinnerton, D., Pearson, K.G., Hood, M.L., 1988. Steady State post-Dryout Experiments at Low Quality and Medium Pressure. UKAEA Report AEEW-R2192.

Takenaka, N., Fujii, T., Akagawa, K., Nishida, K., 1989. Flow pattern transition and heat transfer of inverted annular flow. Int. J. Multiphase Flow 15, 767–785.